

The user who studies the tables in detail will find that the scatter in the values of t_p and ω apparently exceeds a level compatible with even a reduced accuracy of 500 m. This fact originates in the low eccentricity of the orbits and is of no consequence when computing the satellite position. The position of the satellite at a particular epoch does not depend appreciably upon either t_p or ω alone but depends mostly upon the argument of the latitude at the epoch. If t_p and ω are used to the number of figures given in the tables, ignoring their apparent lack of significance, the final computed position will come out all right.

Table 3 Orbital elements of 1962 $\beta\mu$ 1

t_p , days	$10^5 e$	$10^3(i-50^\circ)$ Year = 1962	ω°	Ω°	N
304.3974918	640	0	312.500	54.400	0
305.0488241	615	98	203.758	52.006	9
308.0461184	632	143	212.173	41.122	49
311.0435306	637	144	221.179	30.301	89
313.0669562	648	139	227.989	23.014	116
317.0389895	636	130	242.019	8.672	169
320.1115827	630	129	252.337	357.584	210
327.0061046	628	128	275.123	332.698	302
330.0037612	631	128	285.211	321.881	342
334.0505385	636	127	298.552	307.274	396
338.0223706	646	128	311.613	292.943	449
341.0199277	654	129	321.224	282.126	489
345.0669965	669	128	334.031	267.525	543
348.0640921	681	127	343.336	256.707	583
361.0277845	729	127	21.479	209.919	756
Year = 1963					
2.1723327	749	124	38.855	187.745	838
6.0688138	763	125	49.694	173.683	890
8.0919432	767	124	55.113	166.380	917
10.0401550	772	126	60.393	159.349	943
21.0549804	782	127	89.927	119.598	1090
29.0725571	776	126	111.334	90.660	1197
38.0643095	755	129	135.706	58.212	1317
46.0071787	729	129	157.978	29.543	1423
53.0099960	703	130	178.415	4.126	1517
60.0200170	674	129	199.298	338.974	1610
67.0641389	652	129	221.199	313.557	1704
74.0334930	636	128	243.685	288.405	1797
77.0311392	631	128	253.717	277.583	1837
81.0029996	626	127	266.909	263.249	1890
88.1223456	632	123	290.428	237.561	1965
95.2416236	647	122	313.636	211.862	2080
98.0143516	655	122	322.474	201.854	2117
101.0868377	667	128	332.274	190.757	2158
107.0818016	690	125	350.766	169.127	2238
109.1050647	698	125	356.828	161.826	2265
115.0998296	720	125	14.366	140.188	2345
119.0713077	735	124	25.731	125.856	2398
122.0686210	746	125	34.164	115.039	2438
127.0141314	760	124	47.815	97.191	2504
130.0113809	768	124	55.953	86.374	2544
133.0086333	775	128	64.095	75.559	2584
137.0548896	781	127	74.928	60.961	2638
140.0521176	784	128	82.961	50.145	2678
144.0234590	784	129	93.670	35.810	2731
147.0206828	782	129	101.682	24.994	2771
151.0669463	777	129	112.552	10.390	2825
154.0641910	772	128	120.660	399.574	2865
158.0355579	762	128	131.496	345.240	2918
170.0247691	722	128	165.074	301.970	3078
172.1229345	714	128	171.210	294.397	3106
177.0686404	696	127	185.820	276.548	3172
179.0919256	687	126	191.991	269.246	3199
186.4357616	698	123	214.695	242.749	3297
190.0328267	648	125	226.229	229.762	3345
195.0537940	637	124	242.632	211.640	3412
200.0747790	631	125	259.123	193.519	3479
206.0700164	632	124	278.963	171.884	3559
217.1611167	654	125	315.239	131.861	3707
221.0579333	666	122	327.718	117.796	3759
227.0529284	686	126	346.392	96.160	3839

The computer listings were not designed with these tables in mind, and two hand transcriptions were involved in the final preparation of the tables. There is thus a possibility of typographical error. The author will appreciate it if any apparent errors are called to his attention.

Satellite 1961 $\alpha\eta$ 1 ceased radiating shortly after the 212th day of 1962. The other satellites are still radiating (as of November 18, 1963), but their signals have been of low quality for some time. No accurate orbital elements from Doppler tracking, beyond those given in the tables, can be expected for any of the three. The tables have doubtful accuracy after about day no. 300 of 1962 for satellite 1961 α 1 and after about day no. 200 of 1963 for 1962 $\beta\mu$ 1.

Fission-Fragment-Caused Shear Stress in Gaseous Vortex Reactors

D. B. HARMON* AND E. M. SVATON†
*Douglas Aircraft Company, Inc.,
 Santa Monica, Calif.*

Nomenclature

- D = diameter of gas core containing fissionable materials, cm
 E = total fragment energy through 1 cm² of core boundary, mev
 N = fission fragment number through 1 cm² of boundary in one direction
 p = fragment momentum components perpendicular to 1 cm² of boundary, g-cm/sec-cm²
 R = radius, cm
 \overline{uv} = time-averaged tangential velocity, radial velocity product
 γ = number density ratio of particles to that in standard air
 $\bar{\rho}$ = time-averaged density
 τ = effective shear stress, psf
 τ_w = shear stress at vortex wall

Introduction

CONSIDERABLE work has been performed on gaseous core fission reactors for rocket propulsion uses.¹⁻⁵ Throughout the work that has been performed to date, the assumption has been made that separate solutions of the hydrodynamic and nuclear reactor equations, respectively, are possible; in addition, considerable effort has been expended in computation of the energy carried across the gas core boundary by fission fragments.⁶ It is immediately apparent that a fission fragment has a great amount of momentum. As an adjunct to work on fission fragment energy losses, a subroutine to a computer program was included which calculated, for several different cylindrical gas cores, the momentum carried across any boundary in the core for a preset uranium content and various gas number density ratios compared to atmospheric. The results of these calculations are presented herein, along with a brief discussion of the restrictions on the calculations. The intent of this note is simply to show that fission fragments could cause significant shear stresses in gaseous core nuclear vortex reactors; no attempt is made to solve the problem of the actual shear stress.

Received May 6, 1964. Some of the results presented here were reported verbally during the discussion on Ref. 5 at the Jet Propulsion Laboratory Symposium on Gaseous Fission Reactors, Pasadena, Calif., April 27, 1962.

* Branch Chief, Propulsion Research, Advance Missile Technology, Missile and Space Systems Division.

† Research Engineer, Propulsion Research, Advance Missile Technology; presently Research Engineer, Space Physics and Planetary Sciences, Advance Space Technology, Missile and Space Systems Division.

Discussion

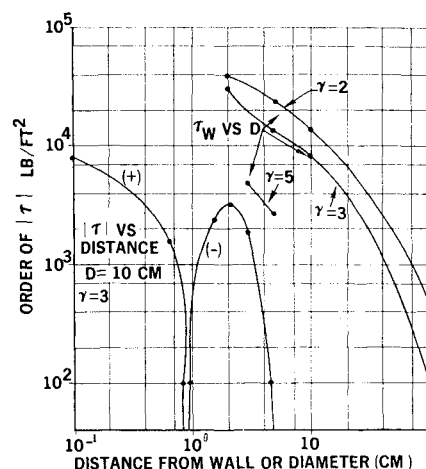
The calculations can be made (using the program) for any given initial distribution of uranium in the vortex. In the results reported here, it has been assumed that the fission fragment number origin corresponds to a certain fraction of the uranium concentration. The uranium content distribution of Ref. 4, with a peak fissionable material concentration of 10^{15} , has been assumed. The fission fragment travel has been computed independently as a function of gas density.⁶ The number of fragments crossing a differential area on the wall of a cylinder is computed assuming a radius of travel equal to the fission fragment path length and an infinitely long cylinder. Since the fission fragment travel is a few centimeters, this radius assumption is totally unrealistic for some of the cylinders considered.

The total energy and component of momentum perpendicular to the wall is computed by the forementioned program. Clearly, the momentum perpendicular to the wall is related to the effective shear stress which depends on the local velocity gradient and the slowing-down rate of the fission fragment. In other words, a stress similar to a turbulent Reynolds stress ($\bar{p} \bar{u} \bar{w}$) exists because of the radial travel of the fragments across the tangential velocity field usually calculated to be present in gas cores— independent of the nuclear effects.

In order to get some idea of the magnitude of the effective shear generated by the fission fragments in their travel, a maximum tangential velocity in the gas cores was assumed. A value of 2000 fps was chosen for the outer edge of the cylinder with a linear gradient assumed going to zero at the center of the cylinder. Shear stresses of the order of those shown in Fig. 1 then result. The computed data are given in Tables 1, 2, and 3. It is immediately evident that for the smaller vortices these values are very large, compared with the magnitude of shear stress that one would expect to find in such a vortex, even with highly turbulent flow.

Turbulence would greatly modify the flow distribution from that assumed. Nevertheless, the momentum carried across the flow by the large number of fission fragments

Fig. 1 Solid body rotation assumed with 2000 fps tip speed; τ = shear stress, D = diameter, γ = # density/# density S. T. P.



is so great that the turbulent momentum transport is still small, compared with the fission fragment momentum transport for lower values of gas density, radius, and high velocity. It is emphasized that the pseudo-stresses given here are not those that would actually be present in the gas cores, as assumed. Rather, this simple calculational technique has been used in an attempt to estimate the order of magnitude that such stresses might take in regions of varying fragment concentration.

Conclusion

From the results presented, it can be concluded that uncoupling of the nuclear and hydrodynamic equations in the vortex type of fission reactors is impossible, except perhaps for large, low-velocity gradient cores. Even if a "two-cylinder vortex" type of reactor is considered, it may be very important to consider the interaction effects near the outer edge of the central core, the area in which it is usually considered that fissioning material ceases to exist. In the vortex flow, it is usually assumed that the fissionable material presents a relatively sharp concentration dropoff with radius; this assumption means that a large radial fragment momentum change should exist across the tangential velocity, unless gas density were very high and fissionable material concentration large over only a small central fraction of the inner zone. Further work in this area is recommended, particularly on the analysis of the true stresses generated by the fragment travel.

References

- 1 Kerrebrock, J. L. and Meghreblian, R. V., "An analysis of vortex tubes for combined gas-phase fission heating and separation of the fissionable material," Oak Ridge National Laboratory Rept. CF-57-11-3, Revision 1 (declassified February 4, 1960).
- 2 Rosenzweig, M. L., Lewellen, W. S., and Kerrebrock, J. L., "The feasibility of turbulent vortex containment in the gaseous fission rocket," ARS J. **31**, 873-883 (1961).
- 3 Kerrebrock, J. L. and Lafyatis, P. G., "Analytical study of some aspects of vortex tubes for gas-phase fission heating," Oak Ridge National Laboratory Rept. CF-58-7-4 (declassified September 2, 1960).
- 4 Grey, J., "A gaseous core nuclear rocket utilizing hydrodynamic containment of fissionable material," ARS Preprint 848-59.
- 5 Wahl, B. W., Strobel, G. L., and Svaton, E. M., "Radiative transfer in inhomogeneous cylindrical gas core nuclear reactors," Jet Propulsion Lab. Symposium on Gaseous Fission Reactors, Pasadena, Calif. (April 27, 1962).
- 6 Wahl, B. W. and E. M. Svaton, "The interaction of fission fragments of uranium with hydrogen, the nature of the expected radiation and some applications to gaseous core vortex systems," Douglas Aircraft Co., Inc., Santa Monica Rept. SM-38621 (October 1961).

Table 1 Light fission fragments

	E , mev	p	N	D , cm	τ
$\gamma = 2$	8.2×10^{14}	310	1.9×10^{13}	2	39,370
	1.8×10^{15}	480	6.6×10^{13}	5	24,384
	3.5×10^{15}	590	1.2×10^{14}	10	14,986
$\gamma = 3$	2.0×10^{15}	160	1.0×10^{14}	100	406
	3.8×10^{14}	240	1.3×10^{13}	2	30,480
	6.8×10^{14}	270	2.4×10^{13}	5	13,716
	1.2×10^{15}	340	4.7×10^{13}	10	8636
$\gamma = 5$	3.8×10^{14}	32	1.8×10^{13}	100	81
		57		3	4826
		54		5	2743

Table 2 Heavy fission fragments

	E , mev	p	N	D , cm	τ
$\gamma = 3$	1.8×10^{14}	200	1.0×10^{13}	2	25,400
	3.4×10^{14}	220	1.7×10^{13}	5	11,760
	5.6×10^{14}	260	3.3×10^{13}	10	6604

Table 3 Light fission fragments; + is toward center

	R , from boundary, cm	E	p	N	τ
$\gamma = 3$	0.7	-5.8×10^{14}	-83	-2.13×10^{13}	1500
	1.4	8.6×10^{14}	82	1.96×10^{13}	2300
	2.1	1.3×10^{15}	140	4.8×10^{13}	3400
	2.8	6.6×10^{14}	89	4.2×10^{13}	1900